Worawat Sa-ngiamvibool
Mahasarakham University

A 10.7-MHz Fully Balanced, Q-of-267, 103-dB-Dynamic-Range Current-Tunable Gm-C Bandpass Filter

***Abstract**. A 10.7-MHz fully balanced, high-Q, wide-dynamic-range current-tunable Gm-C bandpass filter is presented. The technique is relatively simple based on three fully balanced components, i.e. an adder, a low-Q-based bandpass filter and a differential amplifier. The high-Q factor is possible through a tunable bias current. As a simple example at 10.7 MHz, the paper demonstrates the high-Q factor of 267, the low total output noise of 2.089 μVrms, the 3rd-order intermodulation-free dynamic range (IMFDR3) of 82.59 dB and the wide dynamic range of 103 dB at 1% IM3. The center frequency is current tunable over 3 orders of magnitude. Comparisons to other 10.7-MHz Gm-C approaches are also included.*

***Streszczenie.** Zaprezentowano strony prądowo filtr zrównoważony 10.7 MHz pasmowy Gm-C. Technologia bazuje na trzech elementach – sumatorze, filtrze pasmowym i wzmacniaczu różnicowym. Osiągnięto dużą dobroć dzięki strojeniu prądowemu. Przedstawiono przykład filtru i porównano z innymi filtrami. (**Strojony filtr pasmowy Gm-C o częstotliwości 10.7 MHz dobroci 267 i dynamice 103 dB**)*

Keywords: 10.7 MHz, fully balanced, high-Q, Gm-C bandpass filter, sensitivities.
Słowa kluczowe: strojony filtr pasmowy, pasmo Gm-C .

Introduction

Bandpass filters are employed in many applications such as in a radio-frequency (RF) filter for image rejection or an intermediate-frequency (IF) filter for channel selection of a wireless receiver. Typically, FM radio receivers require an IF filter set at a center frequency (f0) of 10.7 MHz based on off-chip devices such as discrete ceramic or surface acoustic wave (SAW) components [1,2]. As off-chip filters are bulky and consume more power to drive external devices, the need for possible on-chip filters for fully viable integrated receivers has increasingly been motivated. Recently, attempts at possible on-chip filters have particularly been demonstrated for 10.7-MHz IF filters based on, for example, switched capacitors (SC) [3-8], and Gm-C [9-13] techniques. Such techniques have, however, repeatedly suffered from low quality (Q) factors from 10 to 55, high total noise from 226 to 707 μV_{rms} and limited dynamic ranges from 58 to 68 dB.

In this paper, a 10.7-MHz fully balanced, high-Q, wide-dynamic-range current-tunable Gm-C bandpass filter is introduced using three fully balanced devices, i.e. an adder, a low-Q-based bandpass filter and a differential amplifier. The high-Q factor is possible through a tunable bias current. The technique is demonstrated through an example at 10.7 MHz. Temperature compensation for both the centre frequency and the Q factor are summarised. Other 10.7 MHz Gm-C approaches are also compared.

The proposed high-Q wide-dynamic-range bandpass filter

Figure 1 shows the proposed system realization of a high-Q bandpass filter where the system is relatively simple based on three fully balanced components, i.e. a two-input adder A_D, a low-Q-based bandpass filter $A_{LQ}(s)$ and a differential amplifier A_G. The transfer function of the low-Q-based bandpass filter $A_{LQ}(s)$ can be written as

(1) $$A_{LQ}(s) = \frac{\left(\frac{\omega_o}{Q_{LQ}}\right)s}{s^2 + \frac{\omega_o}{Q_{LQ}}s + \omega_o^{\ 2}}$$

The pass band gain of (1) is $A_{LQ} = 1$ at $s = j\omega_o$ and Q_{LQ} is a relatively low-Q factor of $A_{LQ}(s)$. Consequently, a closed-loop gain $A_{HQ}(s) = v_o/v_{in}$ is given by

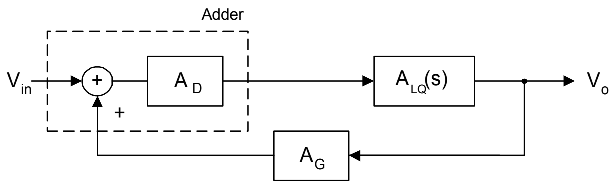

Fig.1. Proposed system realization of a high-Q bandpass filter

(2) $$A_{HQ}(s) = \frac{A_D A_{LQ}(s)}{1 - A_D A_G A_{LQ}(s)}$$

Substituting $A_{LQ}(s)$ in (2) with (1) yields

(3) $$A_{HQ}(s) = \frac{A_D\left(\frac{\omega_o}{Q_{LQ}}\right)s}{s^2 + \frac{\omega_o}{Q_{HQ}}s + \omega_o^{\ 2}}$$

where the quality factor Q_{HQ} is given by

(4) $$Q_{HQ} = \frac{Q_{LQ}}{1 - A_D A_G}$$

It can be seen from (4) that Q_{HQ} may ideally approach infinite if the denominator $(1– A_DA_G)$ approaches zero. In other words,

(5) $$A_G \rightarrow \frac{1}{A_D}$$

In practice, the denominator of (4) may be made relatively small, i.e. A_G is in the proximity of $1/(A_D)$, resulting in a relatively high quality factor Q_{HQ}.

Figure 2 shows the proposed circuit realization for Fig 1 through an example of a fully balanced high-Q current-tunable Gm-C bandpass filter (A_{HQ}). The circuit consists of three fully balanced components, i.e. a two-input adder (A_D), a low-Q-based bandpass filter (A_{LQ}) and a differential amplifier (A_G), using matched npn transistors T1 to T10 and matched pnp transistors T11 and T12. In this case, equation (5) suggests that the gain of the adder $A_D \cong 1$. Firstly, the adder A_D is a modified version of an existing adder [14] and consists of a differential pair (T1, T2), a

common-collector pair (T3, T4) and two current sinks I_1. The 1^{st} small-signal input voltage of A_D is v_{AB} between the bases of T1 and T2 (or nodes A and B). The 2^{nd} small-signal input voltage of A_D is v_{CD} between the bases of T3 and T4 (or nodes C and D). A small-signal output voltage of A_D is v_{EF} between the emitters of T3 and T4 (or nodes E and F).
Secondly, the low-Q-based bandpass filter A_{LQ} is a modified version of an existing low-Q bandpass filter [15] and consists of a differential pair (T5, T6), two capacitors C_1 and $2C_1$, two current sinks I_2 and four loading diode-connected transistors T7 to T10. A small-signal input voltage of A_{LQ} is v_{EF} between the bases of T5 and T6 (or nodes E and F) and is obtained from the output v_{EF} of A_D. A small-signal output voltage of A_{LQ} is v_{GH} between the emitters of T7 and T8 (or nodes G and H). Thirdly, the differential amplifier A_G consists of a differential pair (T11, T12), two resistors R_C and two current sinks I_3. A small-signal input voltage of A_G is v_{GH} between the bases of T11 and T12 (or nodes G and H) and is obtained from the output v_{GH} of A_{LQ}. A small-signal output voltage of A_G is v_{CD} between the emitters of T11 and T12 (or nodes C and D). Finally, the transfer function of the high-Q bandpass filter is $A_{HQ} = v_O / v_{in}$ where $v_{in} = v_{AB}$ and $v_O = v_{GH}$. It can be seen from Fig. 2 that the circuit is fully balanced.

Parameters r_{e1}, r_{e2}, …, r_{e11} and r_{e12} are the small-signal emitter resistance of transistors T1, T2, …, T11 and T12, respectively, where $(r_{e1} = r_{e2}) = V_T/I_1$, $(r_{e3} = r_{e4}) \cong V_T/(\alpha I_1) \cong r_{e1}/\alpha$, $(r_{e5} = r_{e6}) = V_T/I_2$, $(r_{e7} = r_{e8} = r_{e9} = r_{e10}) \cong V_T/(\alpha I_2) \cong r_{e5}/\alpha$, $(r_{e11} = r_{e12}) = V_T/I_3$ for $\alpha = \beta/(\beta+1)$ and β is the common-emitter current gain of a BJT. The usual thermal voltage V_T is approximately 25 mV associated with an pn junction at room temperature.

Firstly, the two-input adder A_D is considered. The output v_{EF} of A_D is obtained through superposition, i.e. $v_{EF} = v_{O1}+ v_{O2}$. The voltage v_{O1} is the output v_{EF} of A_D when the 1^{st}-input v_{AB} of A_D is activated, i.e. $v_{AB} = v_{in}$, but the 2^{nd}-input v_{CD} of A_D is temporary deactivated or separately connected to an ac ground, i.e. $v_{CD} = 0$. In contrast, the voltage v_{O2} is the output v_{EF} of A_D when the 2^{nd}-input v_{CD} of A_D is activated, i.e. $v_{CD} = v_O$, but the 1^{st}-input v_{AB} of A_D is temporary deactivated or connected to an ac ground, i.e. $v_{AB} = v_{in} = 0$. On the one hand, v_{O1} can be found at $v_{CD} = 0$. Therefore, v_{in} of A_D enables a small-signal emitter current $i_{e1} = v_{in}/(2r_{e1})$ passing through the emitters of T1 and T2. The resulting small-signal collector current of T1 and T2 is $i_{c1}=\alpha i_{e1}$. Most of i_{c1} passes through a loading impedance $Z_1 = 2r_{e3}$ formed by T3 and T4. As $v_{O1}\cong i_{c1}Z_1$, therefore $v_{O1}/v_{in} \cong 1$.Consequently, $v_{O1}\cong v_{in}$. On the other hand, v_{O2} can be found at $v_{in} = 0$. Therefore, the gain of the common-collector pair (T3, T4) is $v_{O2} / v_{CD} \cong 1$, or $v_{O2} \cong v_{CD}$. Consequently, $v_{EF} = v_{O1} + v_{O2}$, i.e. the gain of the adder $A_D \cong 1$. As $v_{in} = v_{O1}$ and $v_{CD} = v_{O2}$, therefore

(6)
$$v_{EF} \cong v_{in} + v_{CD}$$

Secondly, the low-Q-based bandpass filter A_{LQ} is considered. The input v_{EF} of A_{LQ} enables a small-signal emitter current $i_{e2} = v_{EF}\,(2sC_1)/(1+s\tau_1)$ passing through the emitters of T5 and T6, where $\tau_1 = 4r_{e5}C_1$. The resulting small-signal collector current of T5 and T6 is $i_{c2} = \alpha i_{e2}$. Most of i_{c2} passes through a loading impedance $Z_2 = 4r_{e7}/(1+s\tau_2)$ formed by T7 to T10 where $\tau_2 = 4r_{e7}C_1$ and therefore $\tau_2 \cong \tau_1/\alpha$. The resulting output of A_{LQ} is $v_{GH} \cong i_{c2}Z_2$, therefore $A_{LQ} = v_{GH} / v_{EF} = v_O / v_{EF}$ represents a low-Q-based bandpass filter A_{LQ} of the form

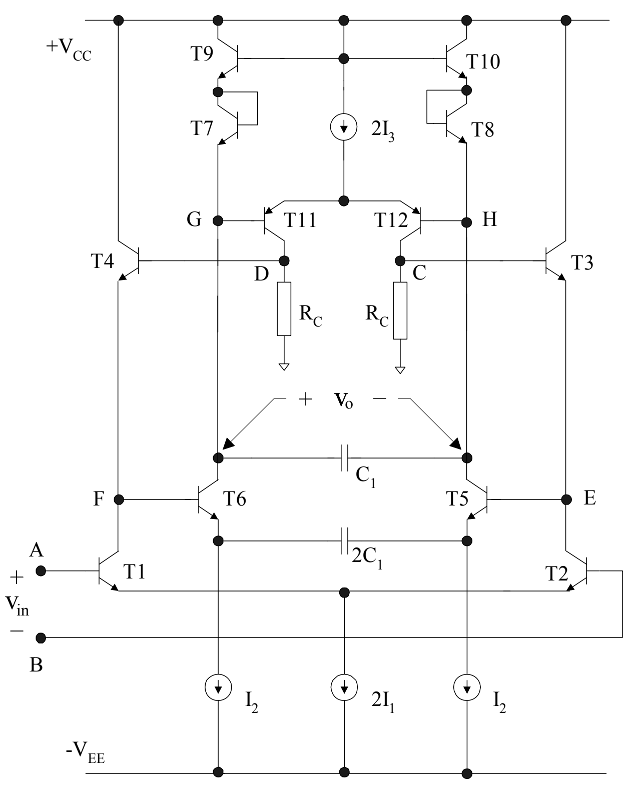

Fig.2. Proposed circuit realization of a high-Q bandpass filter

(7)
$$A_{LQ} = \frac{v_O}{v_{EF}} = \frac{2s\alpha/\tau_1}{s^2 + (1+\alpha)\frac{s}{\tau_1} + \frac{\alpha}{\tau_1^2}}$$

The quality factor of (7) is $Q_{LQ} = (\alpha^{1/2}) / (1+\alpha) \cong 0.5$ which is a relatively low value. The center frequency of (7) is $\omega_{LQ} = (\alpha^{1/2})/\tau_1$. At $s = j\omega_{LQ}$, the passband gain of (7) is $A_{LQ} = 2\alpha/ (1+\alpha) \cong 1$.

Thirdly, the differential amplifier A_G is considered. The input v_{GH} of A_G enables a small-signal emitter current $i_{e3} = v_{GH}/(2r_{e11})$ passing through the emitters of (T11, T12). The resulting small-signal collector current of (T11, T12) is $i_{c3} = \alpha i_{e3}$. Most of i_{c3} passes through a loading resistance $Z_3 = 2R_C$. The resulting output of A_G is $v_{CD} \cong i_{c3}Z_3$, and $v_{GH}=v_O$ therefore

(8)
$$A_G = \frac{v_{CD}}{v_O} = \frac{\alpha R_C}{r_{e11}}$$

Finally, the high-Q bandpass filter A_{HQ} can be considered by substituting v_{EF} in (7) with (6) and substituting v_{CD} in (7) with (8), therefore $A_{HQ} = v_O / v_{in} \cong A_{LQ} / (1- A_G A_{LQ})$, i.e.

(9)
$$A_{HQ} = \frac{v_o}{v_{in}} = \frac{2\alpha s/\tau_1}{s^2 + (1+\alpha-2\alpha A_G)\frac{s}{\tau_1} + \frac{\alpha}{\tau_1^2}}$$

The center frequency of (9) is $\omega_{HQ}=(\alpha^{1/2})/\tau_1 = g_{m5}/(\alpha^{1/2}4C_1)$ where the transconductance $g_{m5}= \alpha / r_{e5}$. The center frequency ω_{HQ} is current tunable by I_2 of the form

(10)
$$\omega_{HQ} = \frac{I_2}{4C_1V_T}\sqrt{\frac{\beta}{\beta+1}}$$

The quality factor of (9) is $Q_{HQ} = (\alpha^{1/2}) / (1+ \alpha - 2\alpha A_G)$. As $\alpha \cong 1$, therefore Q_{HQ} is current tunable by I_3 of the form

(11) $$Q_{HQ} \cong \frac{1}{2(1-A_G)} \cong \frac{1}{2(1-\frac{R_C I_3}{V_T})}$$

It may be suggested from (11) that the quality factor Q_{HQ} ideally approaches infinite at $I_3 = V_T/R_C$. In practice, however, Q_{HQ} should be current tunable to a relatively large value through I_3 where I_3 is in the proximity of V_T/R_C. As an example, it can be expected from (11) that Q_{HQ}=267 if A_G=0.9982, R_C=50 Ω, V_T=25 mV and I_3= 499 μA. At s = $j\omega_{HQ}$, the passband gain of (9) is ideally (i.e. without loading effect and α=1) $A_{HQ} = 1 / (1-A_G) \cong 2Q_{HQ}$ which is much greater than the passband gain of (7) where $A_{LQ} = 2\alpha / (1+\alpha) \cong 1$ at s = $j\omega_{LQ}$.

Sensitivities

Generally, a sensitivity of y to a variation of x is given by S^{y}_{x} = [∂y/∂x][x/y)] where y is a parameter of interest and x is a parameter of variation. Table 1 shows the sensitivity S^{y}_{x} where (x, y) = (C_1, ω_{HQ}), (V_T, ω_{HQ}), (I_2, ω_{HQ}), (β, ω_{HQ}), (R_C, Q_{HQ}), (V_T, Q_{HQ}) or (I_3, Q_{HQ}). It can be seen from Table 1 that the sensitivity of ω_{HQ} to the variations of C_1, V_T, or I_2 are desirably independent of parameters. In addition, the sensitivity of ω_{HQ} to the variation of β is inverse proportional to β, and is a particularly low value (<< 1) when β is large. Therefore, the sensitivity of ω_{HQ} is between –1 and 1. For high-Q realizations ($I_3 \cong V_T/R_C$), the sensitivities of Q_{HQ} to the variations of R_C, V_T, or I_3 are in the same order as those given in the literature [16,17].

Table 1. Sensitivities

$S^{\omega_{HQ}}_{C_1,V_T}$	$S^{\omega_{HQ}}_{I_2}$	$S^{\omega_{HQ}}_{\beta}$	$S^{Q_{HQ}}_{R_C}$	$S^{Q_{HQ}}_{V_T,I_3}$
-1.0	1.0	1/[2(β+1)]	$-2Q_{HQ}$	$2Q_{HQ}$

Dynamic ranges

Dynamic ranges (DRs) of either a specific biquad or an optimized high-Q biquad in a general way have been presented [18]. An expression for the dynamic range of a second-order Gm-C biquad in a general way is given by [18]:

(12) $$DR = \frac{v^2_{\max}}{\overline{v^2_{noise}}} = \frac{v^2_{\max}}{kT\xi Q\left(\frac{1}{C_a}+\frac{1}{C_b}\right)}$$

where $v_{\max}$ is the maximal signal level (at the input or output of a system), $\overline{v^2_{noise}}$ is the mean squared noise voltage at the same point, C_a and C_b are two capacitors in the filter, k is the Boltzmann's constant, T is the absolute temperature, ξ is the noise factor of the transconductor (Gm) and Q is the quality factor. The dynamic range of the proposed technique can be improved by not only increasing $v^2_{\max}$, but also reducing $\overline{v^2_{noise}}$ of (12) as follows. n the one hand, it is known that, the maximal signal level v_{max} of a fully balance circuit is typically twice the maximal signal level v_M of a single-ended circuit [18], i.e. $v_{max} \cong 2v_M$. In other words, the magnitude v_{max} of (12) may be double through the use of a fully balanced circuit. On the other hand, the mean squared noise voltage can be reduced through the use of a shunt positive feedback configuration providing enhanced current gain and thereby improving the overall noise [19]. Table 2 summarizes values of C_a, C_b, and dynamic ranges (DRs) of the proposed Gm-C techniques and other existing Gm-C approaches [18, 20].

It can be seen from Table 2 that if $v_{M1} = v_{M2} = v_{M3}$ and $(KT\xi Q)_1 = (KT\xi Q)_2 = (KT\xi Q)_3$, then $DR_1 > DR_2 > DR_3$. The proposed Gm-C fully-balanced technique can therefore enable a higher dynamic range DR_1, especially when $\overline{v^2_{noise}}$ is also additionally reduced. In particular, as the quality factor Q in (11) becomes Q_{HQ} which is no longer a function of variables such as a center frequency, the dynamic range DR_1 is therefore, unlike existing approaches [18, 20], no longer strongly affected by those variables previously associated in the Q factor. As an example, it can be expected from Table 2 that DR_1 = 105.72 dB if v_{max} = 2 v_{M1} = 288 mV (i.e. -5 dBm through a 50-Ω load), v_{M1} = 144 mV, $kT\xi = 8.33\times10^{-25}$ [20], Q = 267 and C = 150 pF.

Table 2. Dynamic ranges

Refs	Capacitors	v_{max}	$DR = \frac{v^2_{\max}}{(kT\xi Q)\left(\frac{1}{C_a}+\frac{1}{C_b}\right)}$
This paper (fully balanced)	C_a = C C_b= 2C	$2v_{M1}$	$DR_1 = 2.67\frac{v^2_{M1}C}{(kT\xi Q)_1}$
[20] (single ended)	C_a = C C_b= 2C	v_{M2}	$DR_2 = 0.50\frac{v^2_{M2}C}{(kT\xi Q)_2}$
[18] (single ended)	C_a = C C_b= 2C	v_{M3}	$DR_3 = 0.25\frac{v^2_{M3}C}{(kT\xi Q)_3}$

Experimental Results

As a simple example, all transistors in Fig. 2 are modeled by a simple transistor 2N2222 and 2N2907 where the average transition frequency (f_T) is 120 MHz and β is approximately 120 [21]. All current sinks are LM334 [22]. The bias current I_1= I_2= 1.2 mA, I_3= 0.5 mA, R_C=50 Ω and C_1= 150 pF. Figure 3 illustrates the measured frequency response of Fig. 2 at the center frequencies $f_0 = \omega_{HQ}/(2\pi)$ = 10.7 MHz. It can be seen from Fig. 3 that the bandwidth (BW) is 2×20 = 40 kHz and therefore the measured quality factor Q_{HQ} (=f_0/BW) is relatively high at approximately 267.

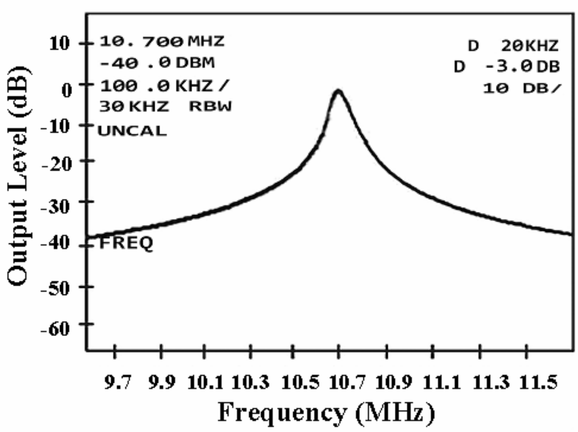

Fig.3. A measured frequency response at the centre frequency $f_0 = \omega_{HQ}/(2\pi)$ = 10.7 MHz and Q_{HQ} = 267.

Figure 4 shows plots of the center frequencies $f_0 = \omega_{HQ}/(2\pi)$ and the corresponding quality factor Q_{HQ} of Fig. 2 versus the bias current I_2 for three cases, i.e. the analysis, the SPICE simulations, and the experimental results. It can be seen from Fig. 4 that f_0 is current tunable over 3 orders of magnitude. As expected, Q_{HQ} essentially remains almost constant at approximately 267 and is, unlike existing approaches, independent of variables such as a center frequency. When I_2 > 1 mA, f_0 drops with further increase of the bias current due to effects of parasitic capacitances at higher frequencies. Although the upper value of I_2 can be expected to be higher than 10 mA, the upper limit of the circuit prototypes has been set to 5 mA, for save operation of the current sources.

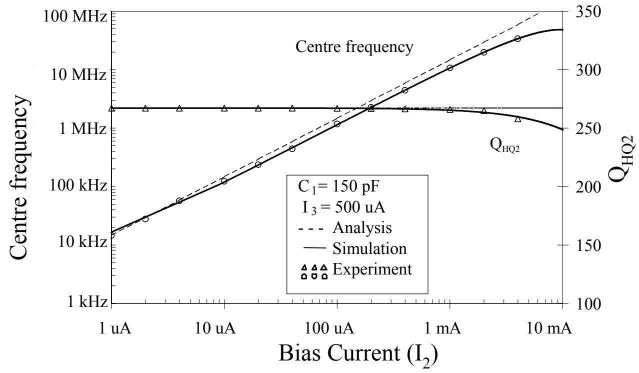

Fig.4. Plots of the center frequency $f_0 = \omega_{HQ}/(2\pi)$ and the quality factor Q_{HQ} versus the bias current I_2.

Low noise performance

Figure 5 shows the measured output noise spectrum shaped by the transfer function of the filter, where the power noise density P_{N1} is relatively low at –153.6 dBm/Hz and the resolution bandwidth (RBW) is at 200 kHz. Table 3 summarizes resulting noise parameters in terms of (1) the resolution bandwidth, (2) the noise density and (3) the total noise. Table 3 concludes that the output noise density V_{N1} = 0.0046 $\mu V_{rms}/\sqrt{Hz}$, the total output noise V_{N3} = 2.0893 μV_{rms} and the total noise power P_{N3} = -100.59 dBm.

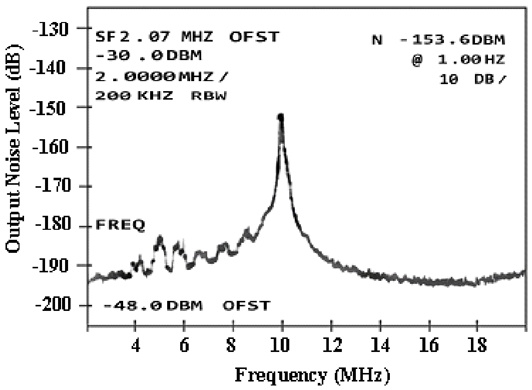

Fig.5. Measured output noise spectrum.

Table 3. Summaries of related noise parameters obtained from Figure. 5

Noise Parameters				Values	Units
1	Resolution bandwidth (RBW)			200	kHz
2	Noise density	P_{N1}	10 log (P_{N2}/1mW)	-153.6	dBm/Hz
		P_{N1}	-	4.3652×10^-19	W/Hz
		v_N^2	P_{N2} × (50 Ω)	2.1826×10^-17	V²/Hz
		v_{N1}	$\sqrt{v_N^2}$	4.6718×10^-9	$V_{rms}/\sqrt{Hz}$
3	Total Noise	V_{N2}	V_N^2 × RBW	4.3652×10^-12	V²
		V_{N3}	$\sqrt{V_{N2}}$	2.0893×10^-6	V_{rms}
		P_{N3}	$10 \log \frac{V_{N3}^2}{(50\Omega)(1\,mW)}$	-100.59	dBm

Wide dynamic range

The circuit is excited with two sinusoids at frequencies $f_1 = f_0$ -7.5 kHz = 10.6925 MHz, and $f_2 = f_0$ + 7.5 kHz = 10.7075 MHz. The 3rd-order intermodulation(IM_3) products $|2f_1-f_2|$ and $|2f_2-f_1|$ are 10.6775 and 10.7225 MHz, respectively.

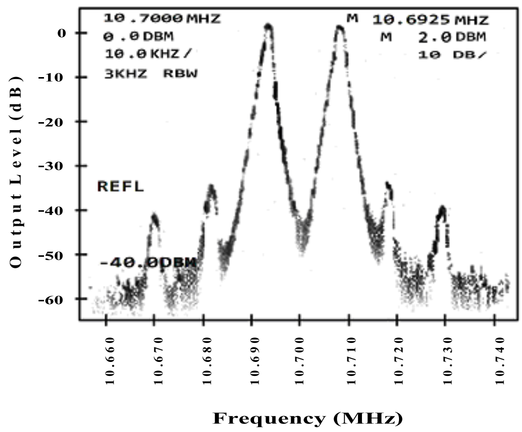

Fig.6. Measured output noise spectrum

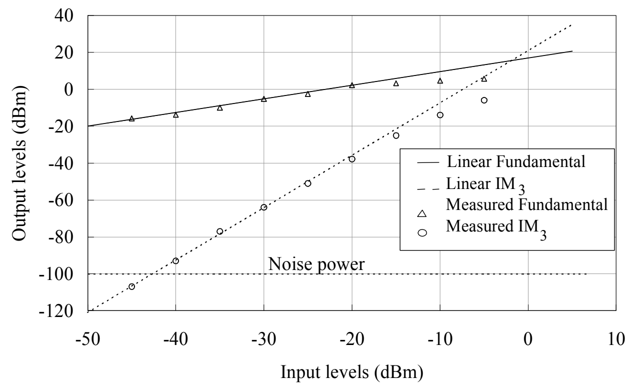

Fig.7. Measured output levels of the fundamental at f_1 and the IM_3 at $|2f_1-f_2|$ versus input levels.

Figure 6 shows the measured output spectrums at Q_{HQ} = 267 using the two-frequency excitation of -20 dBm at f_1 and f_2. It can be seen that the IM_3 products are approximately 40 dB down from the fundamentals and correspond to 1% (or 1% IM_3). Through a 50-Ω load of the spectrum analyzer without the output buffer, Figure 7 depicts the measured output levels (dBm) of the fundamental at f_1 and the IM_3 at $|2f_1-f_2|$ versus the input levels (dBm). It can be seen from Fig. 7 that the noise power P_{N3} = –100.59 dBm. At the input level of □–45 dBm, the output level of f_1 is –18 dBm whilst the output leve of the IM_3 is adjacent to P_{N3} (or intermodulation free). Therefore the 3rd-order intermodulation-free dynamic range ($IMFDR_3$) = (–18 dBm) – (–100.59 dBm) = 82.59 dB. In addition, at the input level of –20 dBm, the output level of f_1 is 2.2 dBm, whilst the output level of the IM_3 is 40 dB down from f_1 (or 1% IM_3). Therefore, the wide dynamic range (at 1% IM_3) = (2.2 dBm) –(–100.59 dBm) = 102.79 dB ≈103 dB which is consistent with the expected value DR_1 = 105.71 dB predicted in section of dynamic range.

Effects of Temperature on the Center Frequency

For the high-Q bandpass filter A_{HQ}, Figure 8 shows two cases of the measured variations of the normalized center frequency f_0/(10.7 MHz) versus the ambient temperature (Celsius). The first case is an "uncompensated" case where the effects of temperature on the center frequency f_0 have not been compensated. The second case is a "compensated" case where the effects of temperature on f_0 have been compensated.

The uncompensated case can be demonstrated by taking Fig. 2 into an oven except that the connected two current sinks I_2 are located outside the oven (i.e. the two current sinks I_2 will be independent of the ambient temperature in the oven). It can be seen from Fig. 8 that the normalized frequency of the "uncompensated" case decreases inversely with the ambient temperature (in the oven) as can be expected from (10) where effects of temperature caused by the thermal dependent voltage V_T is in the denominator of (10).

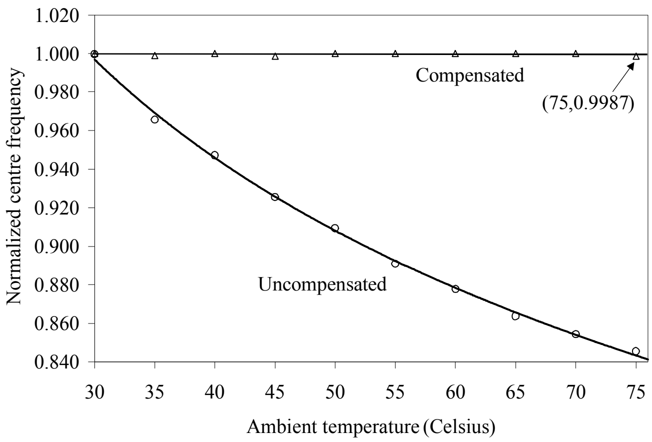

Fig. 8. Normalized centre frequencies versus ambient temperature for the uncompensated and compensated cases.

The compensated case can be demonstrated by taking Fig. 2 into an oven including the connected two current sinks I_2 (i.e. the two current sinks I_2 will also be affected by the ambient temperature in the oven). It can be seen from Fig. 8 that the normalized frequency of the "compensated" case remains relatively constant, as can be expected from (10) where effects of temperature caused by V_T in the denominator of (10) can be compensated by the relatively similar effects caused by V_T of I_2 in the numerator of (10), i.e. $I_2 \propto v_{BE}$ where $v_{BE} = V_T \ln (I_c/I_s)$, I_c and I_s are the collector and saturation currents of a BJT in LM334.

In the compensated case, the temperature coefficients of the normalized center frequencies decrease drastically. The measured temperature coefficients for ambient temperature ranging from T_1 = 30 °C to T_2 = 75 °C are approximately -29 ppm/°C, i.e. $\cong [f(T_2) - f(T_1)]\times10^6/[f(T_1)\times(T_2-T_1)] = (0.9987-1) \times 10^6 / [(1)(75-30)]$. The measurements have been obtained by putting the two frequency-determining capacitors outside the oven, and the measured temperature coefficients are therefore due to the intrinsic circuit parameters only.

Effects of Temperature on the Quality Factor

Effects of temperature on the quality factor have never clearly been reported. In a similar manner to Section D, Fig. 9 shows two cases of the measured variations of the quality factor Q_{HQ} versus the ambient temperature (Celsius), i.e. the uncompensated and the compensated cases. It can be seen from Fig. 9 that Q_{HQ} in the "uncompensated" case increases versus the ambient temperature as can be expected from (11) where effects of temperature caused by the thermal dependent voltage V_T is in the denominator of (11).

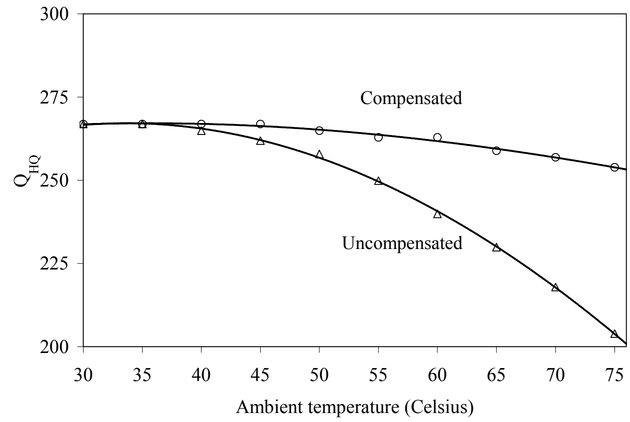

Fig. 9. The quality factor Q_{HQ} versus ambient temperature for the uncompensated and compensated cases

Unlike the two cases in Fig. 8 where the temperature dependent capacitors are located outside the oven, both cases in Fig. 9 have been obtained by including the temperature dependent resistors $2R_c$ inside the oven. It may be observed from both cases in Fig. 9 that the uncompensated effects of the ambient temperature due to the resistor R_c in the numerator of the ratio R_cI_3/V_T in (11) remain evident.

Possible On-Chip High-Q Wide-Dynamic-Range Bandpass Filter

Preferable requirements for an on-chip integrated bandpass filter include low power consumption, low silicon areas of capacitors, high dynamic ranges and high center frequencies whilst maintaining high quality factors. On the one hand, equation (10) suggests that not only the power consumption (P_C) due to I_2 but also the silicon areas due to C_1, can be simultaneously reduced for the same ratio of (10). On the other hand, equation (12) suggests that the smaller the values of the capacitance in the circuit, the smaller the value of the dynamic range (DR). As a result, higher dynamic ranges on chip require higher power consumptions and more silicon areas of capacitors. As an example at the center frequency f_0 = 10.7 MHz whilst maintaining the high quality factor Q_{HQ} = 267, Fig. 10 predicts preliminary interpolation of a power consumption P_C and a corresponding dynamic range (DR at 1% IM_3) versus the capacitance C_1. It can be seen from Fig. 10 that a higher dynamic range DR = 103 dB requires a higher power consumption P_C = 90 mW at C_1 = 150 pF, whilst a lower DR = 81 dB requires a lower P_C = 0.6 mW at C_1 = 1 pF.

High-frequency performance of the circuit will be limited by the transition frequency (f_T) of the transistor. Equation (10) suggests that a higher, more useful, center frequency can be expected using a smaller value of capacitor C_1 (e.g. using stray capacitances), a higher value of I_2 and a higher f_T (e.g. in the region of several GHz) of better transistors. As a particular example, all transistors in Fig. 2 are modeled by a better transistor BFR90A with higher f_T at 5 GHz [23], β = 120 and the bias currents $I_1 = I_2$ = 1 mA. Figure 11 shows high-frequency performance of Fig. 2 through the analysis and the SPICE simulations in terms of the center frequency and the quality factor Q_{HQ}. In this particular example, Q_{HQ} is maintained relatively high and the upper frequency is limited at approximately 500 MHz at C_1 = 1 pF.

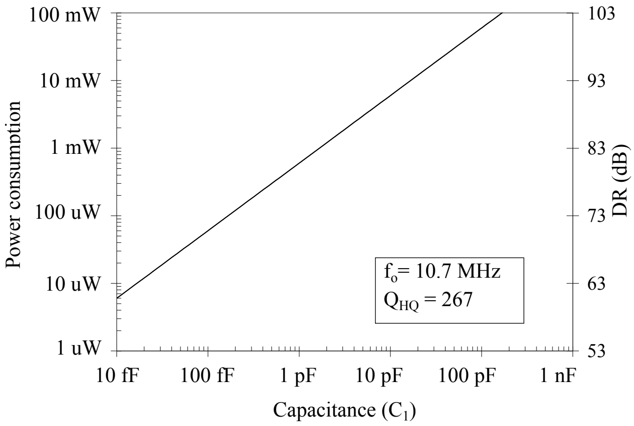

Fig. 10. Preliminary interpolation of the power consumption (P_C) and the dynamic range (DR at 1% IM_3) versus C_1 at f_0 = 10.7 MHz and Q_{HQ} = 267.

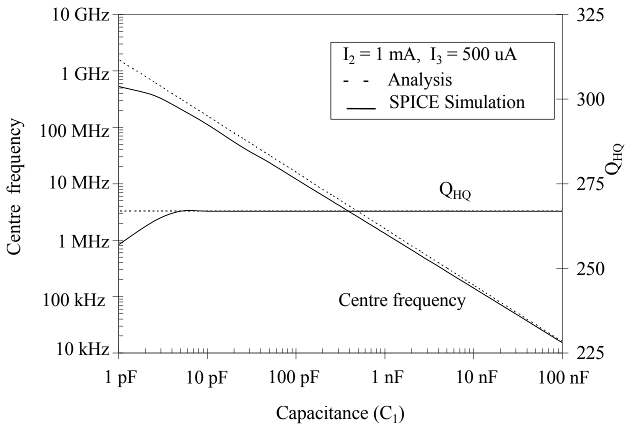

Fig. 11. An example of the center frequencies f_0 and the quality factor Q_{HQ} versus capacitance C_1 with fixed bias currents $I_1 = I_2$ = 1 mA.

Conclusion

A fully-balanced high-Q, wide-dynamic-range current-tunable Gm-C bandpass filter has been proposed based on three simple components, i.e. the adder, low-Q-based bandpass filter and differential amplifier. The high-Q factor is possible through a tunable bias current. An example has been demonstrated at 10.7 MHz for a high-Q factor of 267, the low noise power of –100.59 dBm, the wide dynamic range of 103 dB at 1% IM_3 and the 3^{rd}-order intermodulation-free dynamic range ($IMFDR_3$) of 82.59 dB. The center frequency has been current tunable over 3 orders of magnitude. The proposed technique has offered a potential alternative to a 10.7-MHz high-Q wide-dynamic-range bandpass filter.

REFERENCES

[1] P. J., Quinn., "High-Accuracy Charge-Redistribution SC Video Bandpass Filter in Standard CMOS," IEEE Journal of Solid-State Circuits, 33(1998), no.7, 963-975.

[2] A. E. P.Engelen, J. Plassche, E. Stikvoort, and A. G. Venes, "A Sixth-Order Continuous-Time Bandpass Sigma-Delta Modulator for Digital Radio IF," IEEE Journal of Solid-State Circuits, 34(1999), 1753-1764.

[3] D. Hernandez-Garduno and J. Silva-Martinez, "Continuous-Time Common-Mode Feedback for High-Speed Switched-Capacitor Networks," IEEE J. of Solid-State Circuit, 40(2005), 1610-1617.

[4] J. Silva-Martinez, J. Adut and M. Rocha-Perez, "A 58dB SNR 6th Order Broadband 10.7 MHz SC Ladder Filter," IEEE Custom Integrated Circuits Conference, (2003) 13-16.

[5] S. A. Hammouda, "A 1.5V Opamp Design its High Gain Wide Bandwidth and its Application in a High Q Bandpass Filter Operating at 10.7 MHz," IEEE Trans. on Circuits. and Systems., 38(2002), 185-188.

[6] P. J. Quinn, K. van Hartingsveldt and A. H. M. van Roermund., " A 10.7-MHz CMOS SC Radio IF Filter Using Orthogonal Hardware Modulation," IEEE Journal of Solid-State Circuits., 35(2000), no.12, 1865-1876.

[7] A. Nagsri and G. Nicollini, "A 3 V 10 MHz Pseudo-Differential SC Bandpass Filter Using Gain Enhancement Replica Amplifier," IEEE Journal of Solid-State Circuits, 33(1998). 626-630.

[8] A. Nagari, A. Baschirotto and R. Castello, "A 10.7 MHz BiCMOS High-Q Double-Sampled SC Bandpass Filter," IEEE Journal of Solid-State Circuits, 32(1997), 1491-1498.

[9] A. Tajalli and M. Atarodi, "Design Considerations for a 1.5-V, 10.7-MHz Bandpass Gm-C Filter in a 0.6-um Standard CMOS Technology," IEEE ISCAS'03, 1(2003), I-521 –I-52.

[10] W. Chung-Yu and C. Chung-yun., "The Design of a CMOS IF Bandpass Amplifier with Low Sensitivity to Process and Temperature Variations," IEEE ISCAS 2001, 1(2001), 121-124.

[11] F. Munoz, A. Torralba, R.G. Carvajal, J. Tombs, and J. Ramirez-Angulo, "Floating-Gate-Based Tunable CMOS Low-Voltage Linear Transconductor and Its Applications to HF Gm-C Filter Design," IEEE Trans. on Circuits and Systems-I, 48(2001). no.1, 106-110.

[12] J. Stevenson and S. Edgar, "An Accurate Quality Factor Tuning Scheme for IF and High-Q continuous-time filters," IEEE Journal of Solid-State Circuits, 33(1998), no.12, 1970-1978.

[13] M. Steyaert and J. Silva-Martinnez, "A 10.7 MHz CMOS OTA-R-C Bandpass Filter with 68dB Dynamic Range and on-chip automatic tuning," IEEE Solid-State Cirt. Conference, (1992). 66-67,

[14] B. Srisuchinwong, "Fully Balanced Current-Tunable Sinusoidal Quadrature Oscillator," International J. of Electronics. 87(2000), no. 5, 547-556.

[15] S. Pookaiyaudom, B. Srisuchinwong, and W.Kurutach, "A Current-Tunable Sinusoidal Oscillator," IEEE Trans. Instrumentation and measurement, IM-36(1987), no. 3, 725-729.

[16] D. T. Comer, D. J. Comer and J. R. Gonzzalez, " Ahigh Frequency Integrable Bandpass Filter Configuration," IEEE Trans. Circuit and System II, 44(1997), no. 10, 856-861.

[17] H. Liu and A. Karsilayan, "An Accurate Automatic Tuning Scheme for High-Q Continuous-Time Bandpass Filters Based on Amplitude Comparison," IEEE Trans. Circuit and System II: Analog and Digital Signal Processing, 50(2003), no. 8, 415-423.

[18] G. Groenewold, "The Design of High Dynamic Range Continuous-Time Integratable Bandpass Filters," IEEE Trans. Circuit and System II: Analog and Digital Signal Processing, 38(1991), no. 8, 838-852.

[19] A. Liscidini, M.Brandolini, D. Sanzogni,and R. Castello, A 0.13 μm CMOS front-end, for DCS1800/UMTS/802.11b-g with multiband positive feedback low-noise amplifier," IEEE Journal. of Solid-State Circuits, 41(2006), no. 4, 981-989.

[20] W. B. Kuhn, D. Nobbe, D. Kelly and A. W. Orsborn, "Dynamic Range Performance of On-Chip RF Bandpass Filters," IEEE Trans. Circuit and System II: Analog and Digital Signal Processing, 50(2003), no. 10, 685-694.

[21] Small-Signal Transistor Data, Philips Inc. 2001.

[22] National Semiconductor Data. 2000.

[23] RF Transistor Data, Vishay Semiconductor GmbH. 1999.

The correspondence address is:

Worawat Sa-ngiamvibool, Faculty of Engineering, Mahasarakham University, Tambon Khamriang, Kantharawichai District, Maha Sarakham 44150 Thailand. e-mail: wor_nui@yahoo.com

e-mail: wor_nui@yahoo.com